

We have carried out initial characterization of CcP mutants which include changes at all of the proximal and distal sites that have been suggested to play a role in the facilitation of oxygen-oxygen bond cleavage and compound I formation (with the exception of the proximal histidine).^{2,11} Replacement of the distal histidine residue has the most profound effect, reducing the reaction rate by 5 orders of magnitude. Before we can conclude that this change is due to the loss of catalysis by His-52, we must eliminate such trivial causes for enzyme inactivation as major reorganization of the enzyme structure or changes which block access of hydrogen peroxide to the active site. However, crystallographic structures of CcP(W51F), CcP(W191F), and CcP-(D235N)¹² show that only small, localized structural perturbations occur in these active-site mutants, and we expect the same to be true for CcP(H52L). Nevertheless, a definitive conclusion must await the structure of CcP(H52L). Crystallographic studies of CcP(H52L) are underway.

Acknowledgment. This investigation was supported in part by research grants NSF DMB 87-16459 and PHS 1R15 DK43944 to J.E.E. and L.B.V. and NSF DMB 88-15718 to J.K.; M.A.M. was the recipient of a postdoctoral fellowship from Hemoglobin and Blood Training Grant 5 T32 AM07233-11.

(12) Wang, J.; Mauro, J. M.; Edwards, S. L.; Oatley, S. J.; Fishel, L. A.; Ashford, V. A.; Xuong, Ng. H.; Kraut, J. *Biochemistry* 1990, 29, 7160-7173.

Observation of Triplet-State Electron Spin Resonance in Oxidized C₆₀

Hans Thomann,* Marcelino Bernardo,* and Glen P. Miller*

EXXON Corporate Research Laboratory
Annandale, New Jersey 08801

Received April 20, 1992

The formation, electronic structure, stability, and reactivity of both the reduced and the oxidized C₆₀ fullerene molecules are of intense current interest.^{1,2} Triplet-state ESR spectra have been observed for reduced C₆₀ produced by electrochemical³ and photochemical⁴ methods. ESR spectra of $S = 1/2$ radicals have been reported for C₆₀ dissolved in concentrated and fuming sulfuric acids⁵ and in Magic Acid.⁶ We now report the observation of triplet-state ESR for C₆₀ chemically oxidized in fuming sulfuric acid.

Dissolution of column-purified C₆₀ (>99.9% pure) in fuming sulfuric acid (27% free SO₃) at 263 K with 5% SO₂Cl₂ added to suppress the freezing temperature results in the formation of a green solution. Electron spin echo detected ESR (ESE-ESR) spectra⁷ of oxidized C₆₀ recorded at 100 K are shown in Figure 1. The spectra comprise an overlap of several ESR signals. The most striking feature is the classic Pake absorption pattern characteristic for a randomly oriented triplet ($S = 1$) spin system.⁸

(1) Hammond, G. S.; Kuck, V. J., Eds. *Fullerenes: Synthesis, Properties, and Chemistry of Large Carbon Clusters*; ACS Symposium Series 481; American Chemical Society: Washington, DC, 1992.

(2) McLafferty, F. W., Ed. Special Issue on Buckminsterfullerenes. *Acc. Chem. Res.* 1992, 25, 98-175.

(3) Dubois, D.; Jones, M. T.; Kadish, K. M. *Mater. Res. Soc. Symp. Proc.* 1992, 247, 345.

(4) Wasielewski, M. R.; O'Neil, M. P.; Lykke, K. R.; Pellin, M. J.; Gruen, D. M. *J. Am. Chem. Soc.* 1991, 113, 2774.

(5) Kukolich, S. G.; Huffman, D. R. *Chem. Phys. Lett.* 1991, 182, 263.

(6) Miller, G. P.; Hsu, C. S.; Thomann, H.; Chiang, L. Y.; Bernardo, M. *Mater. Res. Soc. Symp. Proc.* 1992, 247, 293.

(7) ESE-ESR spectra are recorded by plotting the integrated electron spin echo intensity formed following excitation by two short, intense microwave pulses as a function of the applied magnetic field. This produces the direct absorption spectrum rather than the derivative type of display observed in ESR spectra.

(8) Wasserman, E.; Snyder, C. C.; Yeager, W. D. *J. Chem. Phys.* 1964, 41, 1763.

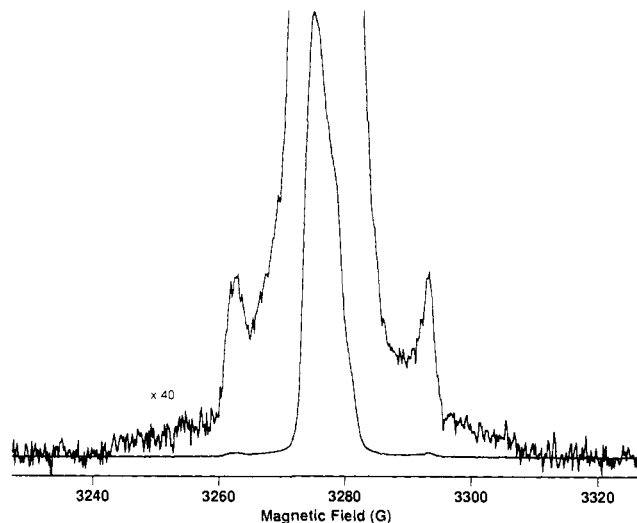


Figure 1. Electron spin echo detected ESR spectrum of C₆₀ in fuming sulfuric acid. Experimental conditions: microwave frequency, 9.1850 GHz; pulse widths, 0.40 and 0.80 μ s; spin echo interpulse delay, 0.45 μ s; pulse sequence repetition rate, 2.5 kHz; temperature, 100 K; sweep width, 100 G; sweep size, 512 points.

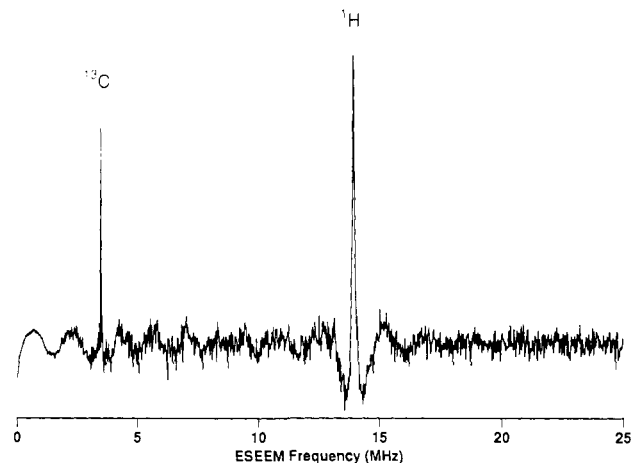


Figure 2. Cosine Fourier transform of the electron spin echo envelope (ESEEM) of C₆₀ in fuming sulfuric acid. Experimental conditions: microwave frequency, 9.185 GHz; pulse widths for stimulated echo, 0.02 μ s; delay between pulses one and two: 0.17 μ s; delay between pulses two and three, from 0.05 to 20.51 μ s; pulse sequence repetition rate, 667 Hz; temperature, 90 K; magnetic field, 3276.1 G.

The zero-field parameter, $|D|$, can be measured directly from the singularities in the EPR spectrum⁹ and yields $|D| = 31$ G.

A strong peak at the ¹³C Larmor frequency was observed in electron spin echo envelope modulation¹⁰ (ESEEM) spectra (Figure 2) of the same sample. Since the C₆₀ molecule is the only source of carbon in the solution, the observation of the ¹³C peak confirms that the $S = 1$ ESR signal arises from the oxidized C₆₀ molecule. The second peak in the ESEEM spectrum is at the proton Larmor frequency. It is attributed to the dipolar coupling of the oxidized C₆₀ radical ion with protons on solvent molecules.

Since ESEEM spectroscopy is most sensitive to weak nuclear hyperfine couplings, pulsed ENDOR^{11,12} spectroscopy was used to search for evidence of larger ¹³C and ¹H hyperfine couplings. As shown in the pulsed ENDOR spectra¹³ of Figure 3, only the

(9) These singularities correspond to resonant field values where the external magnetic field is aligned along the Z or perpendicular to the Z axis of the zero field splitting tensor.

(10) Mims, W. B. *Phys. Rev.* 1972, 5, 2409.

(11) Mims, W. B. *Proc. R. Soc. London* 1965, 283, 452.

(12) Davies, E. R. *Phys. Lett.* 1974, 47A, 1.

(13) Pulsed ENDOR spectra were recorded using the stimulated echo ENDOR technique described by Mims^{10,11} as well as by the inversion recovery technique described by Davies.¹²

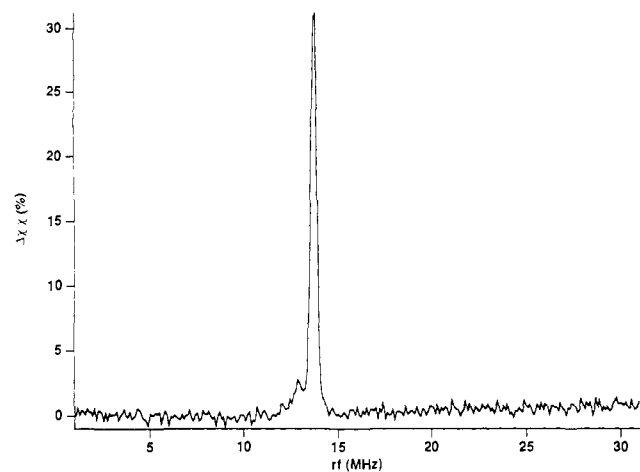


Figure 3. Stimulated echo (also known as Mims) pulsed ENDOR spectrum of C_{60} in fuming sulfuric acid. Experimental conditions: microwave frequency, 9.0250 GHz; magnetic field, 3231.0 G; microwave pulse widths, 0.05 μ s; delay between pulses one and two, 0.30 μ s; rf pulse width, 12.0 μ s; pulse sequence repetition rate, 167 Hz; rf step increment, 0.1 MHz; sweep size, 301 points.

^1H peak from the solvent protons is observed. There is no evidence for larger ^1H or ^{13}C couplings. This rules out the possibility that the shoulders in the ESR spectrum could arise from ^1H or ^{13}C hyperfine interactions.¹⁴ The small peak at the ^{19}F Larmor frequency in Figure 3 arises from the dipolar coupling to SO_2FCl .

The triplet signal intensity reaches a maximum after roughly 2 h while the total integrated ESR susceptibility increases by roughly a factor of 5 after approximately 4 h at room temperature following the initial mixing at 263 K. As a rough estimate, and assuming $S = 1/2$, a maximum of 0.5 spins/ C_{60} is observed. Since the characteristic UV/visible absorptions associated with neutral C_{60} ¹⁵ are not observed at any time, including immediately after the initial mixing at 263 K, the calculated spin density indicates that a significant portion of oxidized C_{60} exists as an ESR-silent (and likely diamagnetic) species. This is consistent with our earlier findings for C_{60} in Magic Acid.⁶

Explanations for the observed triplet-state ESR signal must account for the following experimental observations: a g -value of 2.003; a small (axial) $|D|$ value which is temperature independent between 4 and 110 K; the small ^{13}C hyperfine coupling; and a short electron spin lattice relaxation time, T_{1e} , compared to that observed for the monoradical of C_{60} . Furthermore, assuming that $|D|$ arises from the spin-spin interactions and localized electrons, a first-order approximation for the average distance (r) separating the two electrons,¹⁶ $\langle r \rangle^3 (\text{\AA}) = 6954g^2/|D(G)|$, yields $\langle r \rangle = 9.65 \text{ \AA}$. This is close to the van der Waals radius for the C_{60} molecule¹⁷ and is consistent with two spins on opposite sides of the soccerball cage.¹⁸ The 5-fold-degenerate HOMO of the neutral C_{60} molecule would be expected to undergo a Jahn-Teller distortion after oxidation to the C_{60}^{n+} ion with $n \geq 2$ in a triplet spin state. A Jahn-Teller distortion is consistent with the shorter T_{1e} value observed for the triplet signal. A distortion to an elliptically elongated soccerball structure would also be consistent with the slightly larger $\langle r \rangle$ value.

(14) The weakly coupled ^{13}C nuclei observed in the ESEEM spectrum are not observed in the pulsed ENDOR spectrum because pulse conditions were used to optimize the observation of ^{13}C and ^1H nuclei with larger hyperfine couplings. For details, see: Thomann, H.; Bernardo, M. *Spectroscopy (Ota-awa)* 1990, 8, 119.

(15) Intense band at 330 nm, weak band at 406 nm.

(16) Abragam, A.; Bleaney, B. *Electron Paramagnetic Resonance of Transition Metal Ions*; Clarendon Press: Oxford, 1970; p 492.

(17) (a) Hawkins, J. M.; Meyer, A.; Lewis, T. A.; Loren, S.; Hollander, F. J. *Science* 1991, 252, 312. (b) Fagan, P. J.; Calabrese, J. C.; Malone, B. *Science* 1991, 252, 1160.

(18) The distance between diametrically opposed carbon atoms is ca. 7 \AA . The distance between the carbon π electron cloud on diametrically opposed carbons is roughly 8.5 \AA . This latter distance is the more pertinent number for comparison to the $\langle r \rangle$ value derived from the zero field splitting, $|D|$.

Considering that C_{60} is irreversibly oxidized by electrochemical means with a loss of four electrons,¹⁹ it is tempting to suggest the formation of a Jahn-Teller distorted diradical tetracation with a filled doubly degenerate state below a partially filled triply degenerate HOMO. It is possible, however, that lower oxidation states of C_{60} (e.g., the diradical dication of C_{60} , $C_{60}^{2+,2+}$) are stabilized in the superacid solution and are giving rise to the observed triplet. In either case, the temperature dependence of the EPR signal suggests that the triplet state is the ground state of the C_{60}^{n+} diradical dication. Work continues in our laboratory to sort through these possibilities.

(19) Dubois, D.; Kadish, K. M.; Flanagan, S.; Wilson, L. J. *J. Am. Chem. Soc.* 1991, 113, 7773.

Partial Structures of Maitotoxin, the Most Potent Marine Toxin from Dinoflagellate *Gambierdiscus toxicus*

Michio Murata,[†] Takashi Iwashita,[‡] Akihiro Yokoyama,[†] Masahiro Sasaki,[†] and Takeshi Yasumoto^{*,†}

Faculty of Agriculture, Tohoku University
Tsutsumidori-Amamiyamachi, Aoba-ku
Sendai 981, Japan

Suntory Institute for Bioorganic Research
Shimamoto-cho, Mishima-gum, Osaka 618, Japan

Received April 6, 1992

Maitotoxin (MTX) has been found to be one of the causative toxins of ciguatera, a poisoning caused by ingestion of coral reef fish.¹ In lethal potency (mouse, ip.) MTX exceeds tetrodotoxin by a factor of 200, making it the most potent nonproteinaceous toxin known. The toxin has attracted the attention of biochemists and pharmacologists due to its powerful ability to stimulate Ca^{2+} influx across biomembranes.² Recently, other biological activities were discovered,³ such as phosphoinositide breakdown⁴ and activation of protein kinases,⁵ some of which are not directly linked to elevation of Ca^{2+} levels. As a natural product, MTX is also well-known for its complex structure and molecular weight (3424 Da),⁶ which exceeds that of palytoxin by 748 Da. Thus MTX is one of the most challenging structural targets in natural product chemistry.

Despite our efforts to elucidate the structure of MTX for over 15 years, we have succeeded only in establishing small structural moieties.⁶ In this communication, we wish to report a partial structure of MTX (1) which accounts for 30% of the weight of the molecule.

MTX was extracted from cultured cells of *Gambierdiscus toxicus* and purified as reported previously.⁶ Approximately 25 mg (7.3 μ mol) of MTX was obtained from 5000 L of culture. Extensive measurements of two-dimensional NMR spectra⁷ were carried out, including ^1H - ^1H COSY, 2D HOHAHA, DQF-COSY, NOESY, ^1H - ^{13}C COSY, HMQC, HMBC, and the recent techniques of HSQC and 2D HMQC/HOHAHA. However, overlapping as well as poor resolution of both ^{13}C and ^1H NMR signals due to the large molecular size prevented us from applying routine methods for structural analyses. In particular, the NMR

[†]Tohoku University.

[‡]Suntory Institute for Bioorganic Research.

(1) Yasumoto, T.; Bagnis, R.; Vernoux, J. P. *Bull. Jpn. Soc. Sci. Fish.* 1976, 42, 359-365.

(2) Takahashi, M.; Ohizumi, Y.; Yasumoto, T. *J. Biol. Chem.* 1982, 257, 7287-7289.

(3) Gusovsky, F.; Daly, J. W. *Biochem. Pharmacol.* 1990, 39, 1633-1639.

(4) Berta, P.; Sladeczek, F.; Derancourt, J.; Durand, M.; Travo, P.; Haiech, J. *FEBS Lett.* 1986, 197, 349-352.

(5) Gusovsky, F.; Daly, J. W. Personal communication.

(6) Yokoyama, A.; Murata, M.; Oshima, Y.; Iwashita, T.; Yasumoto, T. *J. Biochem.* 1988, 104, 184-187.

(7) All 2D NMR spectra were recorded either on a GN-500 (500 MHz, General Electric) or a GSX-400 (400 MHz, JEOL) spectrometer except for 2D HMQC-HOHAHA, which was measured on an Omega-500 (500 MHz, General Electric) instrument.